Technical Annex 7.2e–Report on C1 Action

-

Monitoring of composting processes and characterization of compost quality

List of Abbreviation

^{13}C/^{31}P-CPMAS NMR (solid state Cross Polarization Magic Angle Spinning Nuclear Magnetic Resonance on ^{13}C); **CFU**: colony-forming unit; **EC:** electrical conductivity; **FDA**: hydrolase activity with fluorescein diacetate method; **N:** nitrogen; **OC** organic carbon; **OM** organic matter; **thermochemolysis-GC-MS**: off-line thermally assisted hydrolysis and methylation pyrolysis GasChromatography Mass Spectrometry **CMP:** compost from solid digestate-Marco Polo-AGROSELVIT; **SSMP**:fresh solid digestate- Marco Polo-AGROSELVIT; **CV**: on farm compost from project site of CastelVolturno-CERMANU; **L:** on farm composts from LIFE on-farm composting plant of PRIMA LUCE

1.1 Sampling strategies and sample preparation

A sampling strategy was defined in order to perform an adequate analysis and monitoring of both composting processes and chemical quality of the starting organic substrates. Organic matrixes and final compost, representative of lots, were sampled according to procedures extrapolated from the available literature (CEN EN 12579 Rule, 1999; ANPA, 2002).
The following sampling steps were defined taking into account the composting technique used at the "Prima Luce" composting plant, logistics of organic material discharge and their types and volumes:

- picking up at least 5 subsamples (subsample is the amount of material from each taking of the lot in question) from equidistant points of the truck/compost pile (from external and middle areas) and at different depths avoiding the taking from exposed surfaces (sampling below the 10 cm layer). The subsamples for batch were then mixed to form an homogeneous composite sample to be analyzed;
- sampling points have to be more numerous in case of heterogeneous materials;
- mix again the samples manually, if necessary coarsely shredding and drying them on the tray in an oven at about 65°C;
- finely grind the sample with a suitable reel, mix thoroughly and keep in polyethylene containers.

1.2 Composts

The following composts were analysed for the chemical, biological and molecular properties.

Piemonte: project sites Tetto Frati and Grandi, supplier Marco polo company: fresh solid residues (SSMP)and mixed compost (CMP) from bio-digestate process of cow slurries from livestock farms

Campania:

- project site Castel Volturno: on farm mixed compost (CV) from cow and buffalo manure, maize straw, woody fractions from recycled woody boxes
- project sites Prima Luce/Mellone: on farm green compost (L) from

- nutritional/green materials: vegetable residues, from seasonally available crops with high nutritional capacity as easily degradable
- heavy structuring material: ligneous residues from horchard trimming, woody residues from silviculture a and from the final sieving refinement of mature compost

The composition of green and woody fractions (expressed as m3) of the twelve composts achieved from the LIFE on farm composting plant of Prima Luce were as follows:
(L stands for **lot** followed by a number (between 1 and 10) that indicated the composting productive lines and by a letter that identified the various production cycles on the same line)
L1: start 25/07/2014, end 28/10/2014
heavy (ligneous) fraction: (Quercus cerris) Turkey oak 25
nutritional: basil 20; watermelon 15; salads 15; tomato 30
L2 start 30/07/2014, end 29/09/2014
heavy (ligneous) fraction: artichoke 25; Turkey oak 5

nutritional: basil 16; watermelon 25; salads 5

L3 start 30/07/2014, end 21/10/2014

heavy (ligneous) fraction: artichoke 25; Turkey oak 5

nutritional: basil 16; watermelon 25; salads 5

L4 start 24/08/2014. end 14/11/2014

heavy (ligneous) fraction: Turkey oak 40

nutritional: 50; endive, endive scarole, lettuce 30; watermelon, melon, pepper 20

L1A: start 02/09/2014, end 06/11/2014

heavy (ligneous) fraction: 10 (Quercus cerris) Turkey oak

nutritional: lettuce 12,5; endive scarole, salads 22.5; rocket 12.5; pumpkin/watermelon 3.5; basil 11; sorghum 50; solanaceous 9

L2A start 02/10/2014, end 22/12/2014

heavy (ligneous) fraction: Turkey oak 15

nutritional: lettuce 55; endive scarole, salads 104.5; rocket 16.5; pumpkin 2.5; basil 24

L3A start 23/10/2014 end 23/01/2015

heavy (ligneous) fraction: trimming residues 36

nutritional: basil 64; lettuce, endive scarole 103; rocket 16.5; pumpkin 6; broccoli 2

L4A start 13/11/2014, end 19/02/2015

heavy (ligneous) fraction: Turkey oak 16; artichoke 4

nutritional: rocket 152.5; parsley 4; salads 4; tangerine 14

L5/6A start 21/11/2014 end 16/02/2015

heavy (ligneous) fraction: Turkey oak 19; fennel 25

nutritional: rocket 126; salads, endive scarole 28; lettuce 6.5; tangerine 28; broccoli 1,5

L7A start 11/12/2014, end 14/03/2015

heavy (ligneous) fraction: Turkey oak 10; walnut shell 30

nutritional: rocket 104.5; endive scarole, salads 25.5; cabbage, spinach, parsley 6.5; tangerine 14

L7/8 start 30/06/2014, end 05/09/2014

heavy (ligneous) fraction: olive tree trimming 40

nutritional: 50 m3 ; basil, endives, lettuce 50.

L2C start 21/11/2014 end 16/02/2015

heavy (ligneous) fraction: Turkey oak 27; fennel 50

nutritional: rocket 189.5; red chard, cabbage, spinach 7.5; lettuce 2.5; tangerine 7

2 Material and methods

Compost samples were analysed for pH, electrical conductivity, total N, OC, heavy metals (Cadmium-Cd, Chromium-Cr, lead-Pb, Nickel-Ni, Zinc-Zn, Copper-Cu), FDA, total bacteria, fungi, and phytotoxicity/biostimulation and suppressivity on Lepidium sativum, ^{13}C-CPMAS-NMR, Themochemolysis GC-MS

2.1 Chemical analyses

Elemental analyses for C, N and H, were performed with Fisons Elemental Analyzer EA 1108, using Acetanilide as standard reference for instrument calibration.

The determinations of the concentration of total heavy metals were performed on initial organic samples matrices. Analysis were performed on ICP-OES spectrometer (iCAP 6000 Series - Thermo Scientific) following sample mineralization with step-wise acidification process.

2.2 Biological analyses

Basal respiration was from a compost (50-g dry weight) wetted with water up to 80% of its water-holding capacity and placed in a jar (500 ml) with an airtight cap. Released CO2 was measured using a CO2 Analyser IRGA SBA-4 OEM (PP Systems, USA). To evaluate fluorescein diacetate (FDA) hydrolysis, 2.5 g of compost was mixed with 15 ml of 0.2 M potassium phosphate buffered at pH 7.6, followed by the addition of 0.5 ml FDA solution (2 mg ml^{-1}). The mixture was shaken for 2 h in an orbital incubator and the hydrolysis reaction stopped by adding 15 ml CHCl3/ CH3OH (2:1 v/v). The reaction mixture was centrifuged (700×g) and the absorbance of the aqueous supernatant measured at 490 nm.

Populations of fungi, yeast, total bacteria, and pseudomonads were evaluated in by plating serial ten-fold dilutions. Fungi were counted on PDA (Oxoid) pH 6, to which 150 mg L−1of nalidixic acid and150 mg L−1of streptomycin were added. Yeast was counted onrosebengal medium (Oxoid) 32 g L−1, to which 0.1 g L−1of chloram-phenicol (Oxoid) was added.Total bacteria were counted on selective medium (glucose1 g L^{-1}, proteose peptone 3 g L^{-1}, yeast extract 1g L^{-1}, K_2PO_4 1g L^{-1}, agar 15g L^{-1}) to which actidione (cycloheximide)100 mg $L^{-1}$was added. Pseudomonads were counted on selectiveagar medium without iron, to which actidione was added. Finally, spore-forming bacteria were counted onNutrient Agar using compost preparations previously heated at 90◦C for 10 min. Population densities are reported as logc.f.u. $ml^{-1}$of organic matrices.

The method used for the phytotoxicity assessment will be based on evaluating growth of a test plant (Lepidium sativum) on a mixture containing compost plus a base substrate consisting of sand and peat. The procedure involves the preparation of the base substrate by mixing silica sand and peat in a 1:1 volume ratio. Compost is then be added to the base substrate, at 4 increasing amounts. Each treatment is replicated four times. The different mixtures thus obtained are placed in 2 liter pots containing a bottom layer (1 cm) of expanded clay, to ensure drainage. An unfertilized control treatment (base substrate without compost addition) is also be included. The mixture is covered with a layer of 1 cm of sand where seeds will be posed to germinate, to detect the toxicity only on plant development. The number of seeds per pot is adjusted to ensure the germination of at least 100 seeds per pot. Seeds are covered with layer (1 cm) of perlite. At the end of the vegetative development (about 21 days) plants are cut at the collar to determine biomass yield.

The suppressive capability of different composts towards soil borne pathogens *Rhizoctonia solani* and *Sclerotinia minor* damping-off, was evaluated by pot assays on peat as common horticultural supporting matrices, using Lepidium sativum L. as host plant. Peat was amended with composts at rate of 20% (v/v), with un-amended peat as control.

All bioassays were carried out with sterile (twice autoclaved) and not sterile medium.

Several pathogen isolates were obtained from diseased lettuce (Lactuca sativa L.) (S. minor), and cabbage (Brassica oleracea L.) (R. solani) and maintained on PDA medium. Isolates of each species were preliminarily tested for pathogenicity on lettuce, L. sativum, and showed very similar behavior. Pathogen inocula were prepared as follows: common millet seeds were placed in 0.5 L flasks, saturated with a PDB (potato dextrose broth) solution (1/10 w/w) and twice autoclaved.

Flasks were inoculated with fungi cultured on PDA (potato dextrose agar) for 7 days, and incubated for 21 days at 20 ┘ C. The resulting fungal millet inoculum was air-dried for 3 days, powdered in a mortar, and added at four levels to the potting mixtures. Pathogen inoculums was used at different concentrations (0%, 0.3%, 1% and 3% w/w, dry weight) to test the effect of different inoculum density and to avoid the ‘‘flattening effect” of the results often observed when only one concentration is used. In the controls, non-inoculated common millet prepared as described above was added. Pots (7 cm diameter and 100 ml volume capacity) were filled with the different organic mixtures and sown with 20 *L. sativum seeds cv. Comune (Blumen*), moistened to field capacity and arranged in greenhouse (25 °C) following a complete randomized design. Pot distribution was rearranged randomly every 2 days to avoid the effects of environmental heterogeneity in the greenhouse. After 7 days disease incidence was recorded as percentage of diseased plants. Damping-off percentage was calculated as

$$\%DO = \frac{HPo-HPi}{HPi} \times 100$$

where HPo is the number of healthy plants in the non-inoculated control mixture and HPi is the number of healthy plants in the inoculated potting mixes.

2.3 Molecular characterization

The molecular characterization have been performed by solid state Nuclear Magnetic Resonance (CPMAS-NMR) and off-line thermochemolysis-Gas Chromatografy Mass Spectrometry (THM-GC-MS). The combined application of 13C cross-polarization magic angle spinning nuclear magnetic resonance spectroscopy (13C-CPMAS-NMR), and off-line pyrolysis followed by gas chromatography-mass spectrometry (THM-GC-MS), are updated and powerful tools for the molecular investigation of complex organic materials.

2.3.1 13C CPMAS NMR

The nondestructive NMR techniques provide the distribution of organic carbons in a wide range of different matrices and are properly applied to characterize the composition and transformation, of natural organic materials. Besides the basic distribution of C functionalities, the solid state NMR application allows the implementation of specific experiments dedicated to the evaluation of steric arrangement and conformational behavior of complex materials. In particular the analytical appraisal of specific parameters related to cross polarization dynamics, such as cross-polarization time (*tCH*) and the spin-lattice proton relaxation in the rotating frame ($t1\rho H$), are suitable to evaluate structural properties and modification in complex substrates.

Pyrolysis in the presence of tetramethyl ammonium hydroxide (TMAH) is commonly used to study the detailed molecular composition of either natural and synthetic biopolymers. It involves the cleavage of covalent bonds combined with the solvolysis and methylation of ester and ether groups, in complex mixture of organic macromolecules and biopolymers, thereby enhancing the thermal stability of acidic, alcoholic, and phenolic groups and allowing a suitable chromatographic detection of pyrolytic products.

Fine-powdered composite samples of bulk compost samples, were analyzed by solid-state NMR spectroscopy (13C CPMAS NMR) on a Bruker AV300 Spectrometer equipped with a 4 mm

wide-bore MAS probe. The NMR spectra of initial and composted substrates were obtained by applying the following parameters: 13,000 Hz of rotor spin rate; 2 s of recycle time; 1H-power for CP 92.16 W: 1H 90° pulse 2.85 μs; 13C power for CP 150,4 W; 0.5 to 2 ms of contact time; 30 ms of acquisition time; 4000 scans. Samples were packed in 4 mm zirconium rotors with Kel-F caps. The cross-polarization pulse sequence was applied with a composite shaped "ramp" pulse on 1H channel in order to account for the inhomogeneity of Hartmann-Hann condition at high rotor spin frequency. The Fourier transform was performed with 4k data point and an exponential apodization of 100Hz of line broadening. Solid-state 13C Nuclear Magnetic Resonance (NMR) is a powerful tool for non destructive study of solid samples. The analysis of solid materials, however, implies the occurrence of unavoidable technical drawbacks, such as chemical shield anisotropy and dipolar coupling effects, with a loss of signal resolution. Although the application of Magic Angle spinning and high power decoupling, produce a significant improvement of spectral quality, the solid state spectra of organic materials are characterized by a large signal broadening and an overlapping of carbon functionalities. As a consequence, the main natural organic components, are conventionally grouped into the following chemical shift regions: Alkyl-C: 0-45 ppm; Methoxyl-C/C-N: 45-60 ppm; O-Alkyl-C: 60-110 ppm; Aromatic-C: 110-145 ppm; O-Aromatic-C: 145-160 ppm, and Carboxyl-C: 190-160 ppm. The relative contribution of each region was determined by integration (MestreNova 6.2.0 software, Mestre-lab Research, 2010), and expressed as percentage of the total area. In order to summarize the modification occurring with incubation time, two indices of the extent of decomposition, named Hydrophobic index (HB) and Aromatic ratio (Ar) were determined from the combination of relative area of different NMR spectral regions (Table 2) as follows:

$$HB=\Sigma\,[(0\text{-}45)+1/2(45\text{-}60)+(110\text{-}160)] \,/\, \Sigma\,[1/2(45\text{-}60)+(60\text{-}110)+(160\text{-}190)]$$

$$Ar=\Sigma\,[1/2(45\text{-}60)+(110\text{-}160)] \,/\, \Sigma\,(0\text{-}160)$$

In order to determine the conformational behavior and the best NMR acquisition parameters of complex organic materials, Variable Contact Time (VCT) experiments have been performed on different composts. The analytical conditions were the following:

VCT 13,000 Hz of rotor spin rate; 2 s of recycle time; 92.16W 1H-CP pulse power; Variable contact time: from 0.01 to 10 ms for a total of 20 steps; 30 ms of acquisition time; 2000 scans

The equation used to fit the experimental data and to evaluate the molecular CP parameters was the following:

1) VCT $I=[I0/\alpha]\ x\ [exp\ (-tCP/\ t1\rho H)]\ x\ [1-(exp\ (-\alpha\ tCP/\ tCH)]$

I=experimental signal intensity; I0=theoretical max signal intensity; α=(1-tCH/t1ρH)] tCP=instrumental variable contact time(s); tCH = molecular cross polarization time; t1ρH= molecular proton-lattice relaxation time (in the rotating frame)

2.3.2 Off-line TAHM-GC-MS

For off line-TAHM-GC-MS about 0.2 g of bulk compost samples were placed in a quartz boat with 0.5 mL of TMAH (25% in methanol w/v) solution. After drying under a stream of nitrogen, the mixture was introduced into a Pyrex tubular reactor (50 cm × 3.5 cm i.d.) and heated at 400 °C for 30 min in a circular oven (Barnstead Thermolyne 21100 Furnace, Barnstead International, Dubuque, IA, USA). The gaseous products from thermochemolysis were flowed into two chloroform (50 mL) traps in series, kept in ice/salt baths. The chloroform solutions were combined and rotoevaporated to dryness. The residue was dissolved in 1 mL of chloroform and transferred in

a glass vial for GC-MS analysis. The GC-MS analyses were conducted with a Perkin Elmer Autosystem XL by using a RTX-5MS WCOT capillary column (Restek, 30 m × 0.25 mm; film thickness, 0.25 mm) that was coupled, through a heated transfer line (250 °C), to a PE Turbomass-Gold quadrupole mass spectrometer. The chromatographic separation was achieved with the following temperature program: 60 °C (1 min. isothermal), rate 7 °C min−1 to 320 °C (10 min. isothermal). Helium was used as carrier gas at 1.90 mL min−1, the injector temperature was at 250 °C, and the split-injection mode had a 30 mL min−1 of split flow. Mass spectra were obtained in EI mode (70 eV), scanning in the range 45–650 m/z, with a cycle time of 0.2 s. Compound identification was based on comparison of mass spectra with the NIST-library database, published spectra, and real standards

3 Results

3.1 Chemical analyses

The data related to pH, EC and elemental composition of analyzed composts are shown in Table 1. Almost all the composted materials were characterized by a sub-alkaline or alkaline pH, which ranged from 6.95 to 9.10, characteristic of the increasing concentration of minerals components, such as alkaline metals (e.g. Ca, Mg, K, Na), with the progressive decrease of total dry weigh during the composting processes; the EC ranged from 1.3 to 3 µS cm^{-1} with the exception of the on farm compost from Castel Volturno which showed a largest salt concentration (6.591 µScm^{-1}) may be related to the inclusion of buffalo manure in the starting matrix components.

The solid digestate and the mixed composts made from cattle manure, used in Piemonte (SSMP, CMP) and in the project site of Castel Volturno (CV) showed an larger content of total N in respect to the green composts of Prima Luce, except for the composts L7A (Table 1). This finding is related to the different source of organic materials involved in the composting processes. In fact the large amount of fresh nutritional easily degradable matrices used for the attainment of green compost, may have promoted a larger decomposition of bio-labile components, such as peptide moieties. However no large differences were found in the final C/N ratio which ranged from 18 to 23, a part for the fresh solid digestate which larger OC content raised the C/N ratio to about 27

Table 1 Chemical characteristics of composts

Compost	pH	EC (µS cm^{-1})	OC (%)	N (%)	C/N[a]
SSMP	7.92	1.904	43.8	1.91	26.8
CMP	8.38	2.982	35.1	1.96	20.9
CV	8.57	6.591	34.3	2.0	20.0
L1	7.77	1.722	26.7±0.8	1.30	24.0
L2	8.43	1.316	29.7±1.2	1.28	27.1
L3	9.10	2.639	32.1±0.9	1.55	24.2
L4	8.73	2.258	34.2±2.2	1.76	22.7
L1A	7.73	1.621	23.9±1.3	1.20	23.2
L2A	9.02	1.514	28.9±1.0	1.68	20.1
L3A	8.59	1.564	31.0±3.2	1.52	23.8
L4A	7.00	1.339	30.0±2.1	1.89	18.5

L5/6A	6.95	1.950	25.2±0.6	1.32	22.3
L7A	8.20	2.324	33.0±0.8	2.31	16.7
L7/8	8.82	2.684	26.0±0.5	1.68	18.1
L2C	8.21	1.85	31.8	1.85	20.1

a atomic ratio

All the analyzed compost showed a concentration of heavy metal, below the legal limits fixed for both, green and mixed composted materials (Table 2)

Table 2. Average heavy metals content (mg kg^{-1} dry matter basis) found in fresh materials

Element	Units	Range	law limits *
Cd	mg/kg d.m.	0 - 0.41	1.5
Cr	mg/kg d.m.	0.43 - 5.85	0.5 **
Cu	mg/kg d.m.	2.29 - 21.22	150
Ni	mg/kg d.m.	0.4 - 4.86	50
Pb	mg/kg d.m.	0.66 - 11.52	140
Zn	mg/kg d.m.	2.98 - 122.8	500

*Limits according to – D.lgs. 75/2010 – Composted soil improvers. **Cr VI

3.2 Biological analyses

Notwithstanding the differences among composts all organic matrices showed an effective biological activity as revealed by the total hydrolase properties (FDA) (Table 3). Also different responses were found in the phytotoxicity/biostimulation assays on Lepidium, with all composts revealing a positive effect on the plant development at larger doses concentrations (Table 3)

Table 3. Biological analyses: hydrolase activity (FDA), bioactivity, quantification of total bacteria (Tot B), Pseudomonas-like (Ps Lb) and Bacillus-like bacteria (BLb) and total fungi (TotF).

Compost	FDA (µg g^{-1}d.m)	Biostimulation (%)			Tot B	Ps Lb	BLb	Tot F
		50 g/L[a]	15 g/L[a]	5 g/L[a]	(Log_{10} CFU[b] g^{-1})			
SSMP	16.2	28.7	61.8	44.0	6.0	5.3	4.6	3.8
CMP	6.8	25.3	19.3	5.2	8.8	12.1	5.7	4.2
CV	7.7	25.9	22.6	32.1	6.2	7.2	5.5	4.8
L1	3.2	8.8	17.9	-23.5	8.6	7.8	8.6	4.7
L2	1.8	7.9	-3.7	-13.3	7.9	12.4	6.5	4.2
L3	2.9	23.3	7.8	-0.8	7.5	7.8	6.9	5.9
L4	8.3	34.6	64.4	19.1	12.6	12.6	6.4	5.2
L1A	7.0	140.5	129.1	92.6	8.0	7.8	5.6	6.0
L2A	12.0	44.2	39.4	40.0	6.8	6.7	6.1	3.3
L3A	11.4	9.8	1.5	-7.4	6.6	7.6	5.8	4.0
L4A	2.6	30.9	32.3	32.9	8.1	8.2	5.8	6.0
L5/6A	2.7	12.3	24.9	20.7	8.2	8.2	6.8	5.2
L7A	2.7	12.3	24.9	20.7	5.9	5.7	5.9	5.23
L7/8	3.8	5.6	20.9	-1.2	7.6	7.7	6.8	6.4
L2C	2.7	17.3	0.5	2.2	7.0	7.0	6.3	4.6

a compost doses

b Colony-forming unit

All composts were analysed for concentration of total bacteria and fungi, Pseudomonas spp. and thermal resistant bacteria (such as Bacillus spp.) (Table 3) and for presence or counting of potentially harmfull bacteria, such as Enterobacteria, Clostridium spp., Escherichia coli, Salmonella, total and faecal Coliforms and Streptococcus spp. (Table 4). Total bacteria and fungi ranged from 5.88 to 12.56 and from 3.30 to 6.36 log10 C.F.U. g^{-1} of compost, respectively. Pseudomonas spp. and thermal resistant bacteria ranged from 5.30 to 12.62 and from 4.60 to 8.56 log10 c.f.u. g^{-1} of compost, respectively. No Enterobacteria and no Salmonella were detected in all the compost, whereas total and faecal Coliforms were detected in almost all the composts. Streptococcus were detected only in one compost and Escherichia coli was detected only in three composts. Eight composts containing Clostridium spp.

Table 4. Microbiological analyses: detection of harmful bacteria (*Enterobacteria*- Ent; *Clostridium*-Clos; *Escherichia Coli* E-Coli; *Salmonella*-Sal; *Total Coliform*-TC, *Fecal Coliform*-FC; *Sptreptococcus*-Sptrc)

Compost	Ent	*Clos*	*E. coli*	*Sal*	TC	FC	Sptrc
	(Log_{10} CFU[a] g^{-1})				MPN[b]		
SSMP	0	0	0	0	4.5	0.9	0
CMP	0	0	0	0	4.5	0	0
CV	0	0	0	0	9.5	0	0
L1	0	0	0	0	15.0	0.9	0
L2	0	4.5	0	0	9.5	4.5	0
L3	0	4.0	0	0	25.0	4.5	0
L4	0	0	0	0	140.0	45.0	0
L1A	0	2.6	0	0	9.5	0.4	0
L2A	0	3.7	0	0	0.9	0.4	0
L3A	0	3.4	0	0	0	0	0
L4A	0	3.8	0	0	0.4	0	0
L5/6A	0	0	0	0	7.5	2.5	0
L7A	0	3.2	0	0	9.5	0.9	0
L7/8	0	3.7	0	0	9.5	4.5	0
L2C	0	2.5	0	0	9.5	0	0

a Colony-forming unit
b Most probable number

On farm composts were analyzed for their potential suppressive activity against two "soil-borne" phytopathogenic fungi, *Rhizoctonia solani* and *Sclerotinia minor*, using Lepidium sativum as host plant. Bioassays were carried out under laboratory conditions, in artificially infected soil-peat amended with raw or heat-sterilized compost samples at 20% vol. concentration. The reduction of damping-off disease incidence found in each treatment for all the analysed composted materials, revealed a significative level of disease suppressiveness, , compared with the not-amended controls. The in vivo assays evidenced a differential responses of the fungal infections on seedling among the various examined composts (Fig. 1). The duplication of the bioassays with *R. solani* and *S. minor* on L. sativum using additionally autoclaved composts, allowed to estimate the relative contribution

of the biotic component of the amendment, that was completely eliminated by heating, on the whole suppressive effect displayed by raw samples.

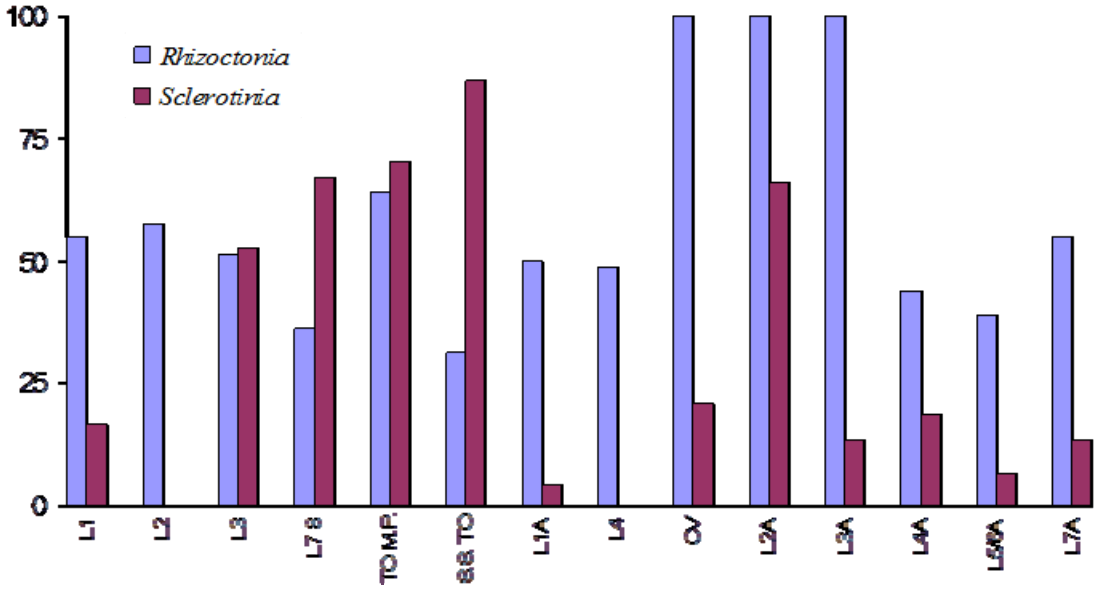

Figure 3. *Compost suppressivity against Rhizoctonia solani and Sclerotinia minor.*

Moreover, the two pathogens helped to differentiate the magnitude and the variability of this peculiar property of on farm composts among both the samples and the pathogens with different aggressiveness. In order to evaluate the plausible mechanisms underlying on farm compost suppressiveness, data of bioassays will be computed in a broad view with all other measured chemical, biochemical and microbiological characteristics of each sample. However, starting a deep investigation of the biological component of composts able to cause pathogen suppression, antagonistic bacteria populations has been isolated, collected and assayed for their in vitro activity against the two model pathogens (Table 5).

Table 5. *Selection of Bacillus-like bacteria for their antibiosis activity against Rhizocotonia solani and Sclerotinia minor.*

Compost	N° Heat-resistant isolates	N° Antagonistic isolates	
		Rhizoctonia	*Sclerotinia*
SSMP	14	13	10
CMP	16	0	0
CV	11	8	8
L1	6	0	0
L2	11	6	7
L3	24	24	5
L4	8	7	6
L1A	14	4	4
L2A	4	1	0

L3A	21	6	9
L4A	17	1	1
L5/6A	6	0	0
L7A	13	7	5
L7/8	19	5	12
L2C	nd	nd	nd

3.3 Molecular characterization

3.3.1 CPMAS 13C NMR analysis

The spectra in Figure 4 show representative VCT experiments carried out to determine the best NMR acquisition parameters for compost samples. A comparable optimum contact time around 1 ms was found for the various organic materials from either manure derived (SSMP, CMP and CV) or green based composts. This fitting value correspond to the average contact time usually applied in NMR analyses of natural organic matter. In fact the proton density associated complex organic matrices allow an averaged spin diffusion among the different molecules thus promoting a common similar cross polarization dynamics.

The NMR spectra of bulk compost are reported in Figures 5a, 5b, 5c

The different resonances in the O-alkyl-C region (60-110 ppm) are currently assigned to monomeric units in oligo and polysaccharide chains of plant tissue . The intense signal around 72 ppm corresponds to the overlapping resonances of carbon 2, 3, and 5 in the pyranoside structures in cellulose and hemicelluloses, whereas the signal at 105 ppm is the specific mark of anomeric carbon 1 of linked glucoses in cellulose. The shoulders at 62/64 and 82/88 ppm represent, respectively, carbon 6 and 4 of carbohydrate rings, the low field resonances (higher chemical shift) of each couple being related to the presence of crystalline forms of cellulose, while the high field ones (lower chemical shift) are typical of amorphous forms and/or hemicellulose structures.

In the alkyl-C interval (0-45 ppm) the shoulder marked by peaks at 19 and 31 ppm, indicated, respectively, the presence of terminal methyl groups of aliphatic chains and that of bulk methylenes (CH2) segments of different lipid molecules, like wax, sterol and cutin components, while the shoulder around 26 ppm is associated with the CH2 group in α and β position of alcoholic portion in aliphatic esters. The less intense and broader signals at 39-40 ppm, are mainly attributable to the inclusion of tertiary (CH) and quaternary (C-R) carbons in assembled rings of sterol derivatives.

The signal at 56 ppm is related to the methoxyl substituent on the aromatic rings of guaiacyl and syringyl units in lignin, with a possible partial contribution of the C-N groups in peptidic moieties.

The broad band included in the 110-130 ppm shift interval, derive from protonated and C-substituted phenyl carbon of lignin monomers, as well as from the typical aromatic moieties in lignans and flavonoids. The slight shoulder shown in the phenolic region (140-160 ppm) indicated the initial lower relative contribution of O-substituted aromatic carbons, pertaining to lignin and lignan components. Finally, the signals in the carbonyl region (190-160 ppm) result from the overlapping of different carboxyl groups related to aliphatic acids, amide groups in amino acid moieties and acetyl substituent in carbohydrates components of hemicelluloses.

The NMR spectra of bulk compost samples, revealed an effective stabilization of organic biomasses, characterized by the relative preservation of recalcitrant molecules. Although the direct correlation of quantitative NMR outcomes with decomposition processes and their extensive application to different organic materials may be questionable, the evaluation of NMR characteristics have revealed to be reliable probing tools to estimate, either, reactivity or recalcitrance of decomposing biomasses such as composts, litters and soil OM inputs. The marked decrease of O-alkyl- carbon atoms (60-110 ppm), combined with the increase of NMR signals associated to alkyl (0-45), aromatic (110-160) and methoxyl (45-60) regions, (Table 6), is in line with the selective preservation of stable hydrophobic organic compounds in final mature composts, currently observed in aerobic composting processes. The degradation of polysaccharide constituents, in final compost samples, was further highlighted by the flattening shown for the shoulders related to the C4 atoms, involved in the glycosidic bond (82-84 ppm), associated with a corresponding broadening of the C1 resonances (104-105 ppm) (Fig. 5), that suggested the progressive breakage of the 1-4 linkage and the consequent shift of the residual unbound carbons to less deshielded position. Moreover, the molecular modification of bulk compost samples, summarized by the structural HB and Ar indexes, confirmed the significant improvement of the overall hydrophobic character associated with the OM stabilization of composting matrices (Table 6).

Table 6 Relative distribution (%) of signal area over chemical shift regions (ppm) in 13C-CPMAS-NMR spectra of initial biomasses (t0) and final bulk compost samples

Samples	190-160	160-145	145-110	110-60	60-45	45-0	HB[a]	Ar[a]
SSMP t0	4.4	4.6	14.3	62.9	7.8	6.1	0.41	18.8
CMP	5.2	4.5	13.7	54.6	10.1	11.8	0.54	18.3
CV t0	8.6	1.6	9.7	59.1	11.1	10.0	0.40	11.3
CV	6.6	3.6	13.7	49.1	11.1	16.0	0.63	17.3
L1 t0	8.4	2.0	6.7	49.6	9.5	23.8	0.64	8.7
L1	6.4	3.0	10.7	37.6	12.5	29.8	0.99	13.7
L2 t0	8.8	2.6	9.1	52.2	10.6	16.6	0.55	11.8
L2	5.8	3.6	12.1	42.2	13.6	22.6	0.82	15.8
L3 t0	9.2	2.8	13.2	56.2	9.8	8.9	0.45	15.9
L3	7.2	4.8	17.2	46.2	9.8	14.9	0.71	21.9
L4 t0	7.1	2.7	12.8	54.9	11.2	11.2	0.52	15.6
L4	5.1	4.7	15.8	46.9	11.2	16.2	0.74	20.6
L1A t0	4.3	1.6	12.3	60.7	8.8	12.2	0.47	13.9
L1A	5.3	4.6	15.3	45.7	11.8	17.2	0.76	19.9
L2A t0	5.6	3.1	12.8	58.5	7.8	13.2	0.51	15.9
L2A	3.6	5.1	16.8	48.5	9.8	16.2	0.75	21.9
L3A t0	5.7	1.6	12.0	52.8	14.0	13.9	0.59	13.6
L3A	4.7	3.6	14.0	43.8	14.0	19.9	0.80	17.6
L4a t0	8.3	1.5	14.0	49.8	11.9	14.6	0.62	15.5
L4A	6.3	3.5	18.0	39.8	11.9	20.6	0.92	21.5
L5/6A t0	6.0	3.6	9.5	60.4	9.1	11.4	0.44	13.1
L5/6A	4.0	3.6	11.5	55.4	11.1	14.4	0.54	15.1
L7A t0	4.6	5.5	18.4	50.9	12.0	8.6	0.69	23.9

L7A	6.6	7.5	21.4	35.9	14.0	14.6	1.02	28.9
L7/8 t0	5.7	2.2	7.9	58.2	10.9	15.1	0.48	10.1
L7/8	6.7	4.2	12.9	41.2	12.9	22.1	0.84	17.1
L2C t0	6.2	2.3	7.4	51.0	8.4	24.6	0.67	9.7
L2C	5.2	3.3	12.4	39.0	11.4	28.6	1.00	15.7

a HB=Σ [(0-45)+1/2(45-60)+(110-160)] / Σ [1/2(45-60)+(60-110)+(160-190)]
Ar=Σ [1/2(45-60)+(110-160)] / Σ (0-160)

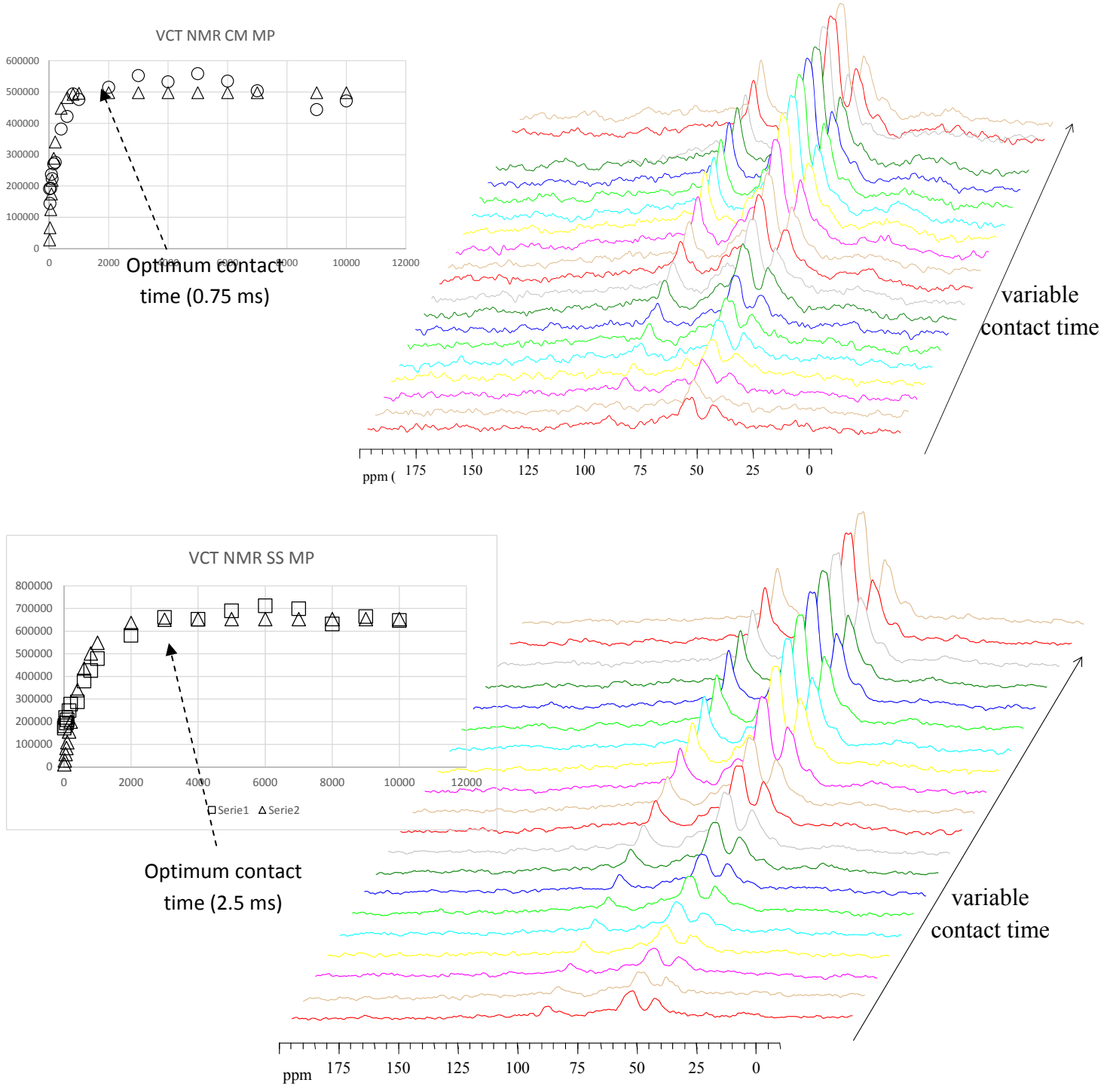

Figure 4 Pseudo bidimensional VCT NMR experiments and VCT curves of SSMP and CMP samples

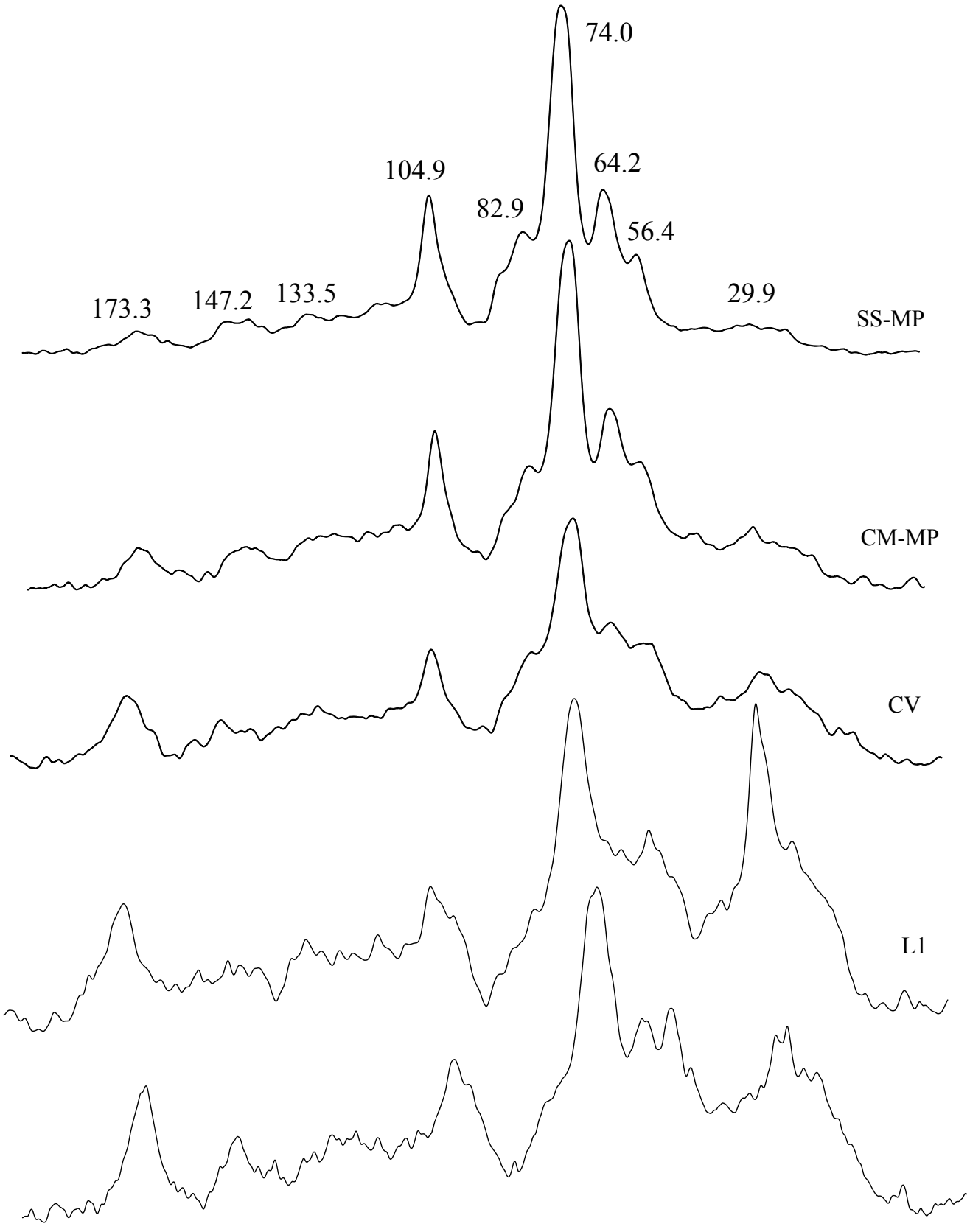
74.0
104.9
64.2
82.9
56.4
173.3
147.2
133.5
29.9
SS-MP
CM-MP
CV
L1

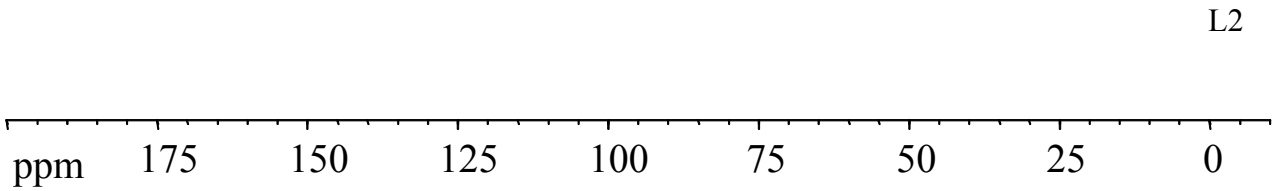

Figure 5a 13C CPMAS spectra of mature compost

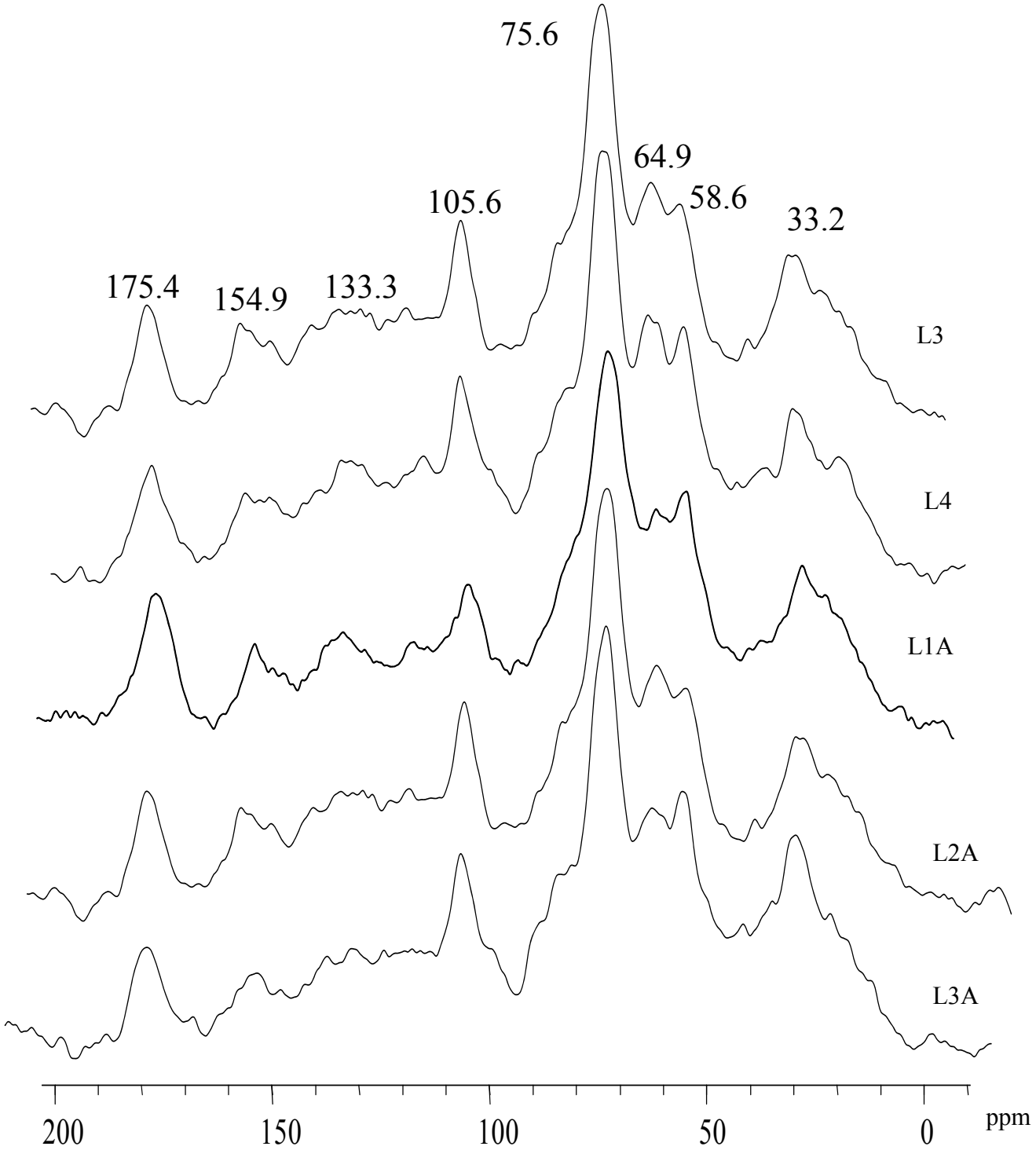

Figure5b 13C CPMAS spectra of mature compost

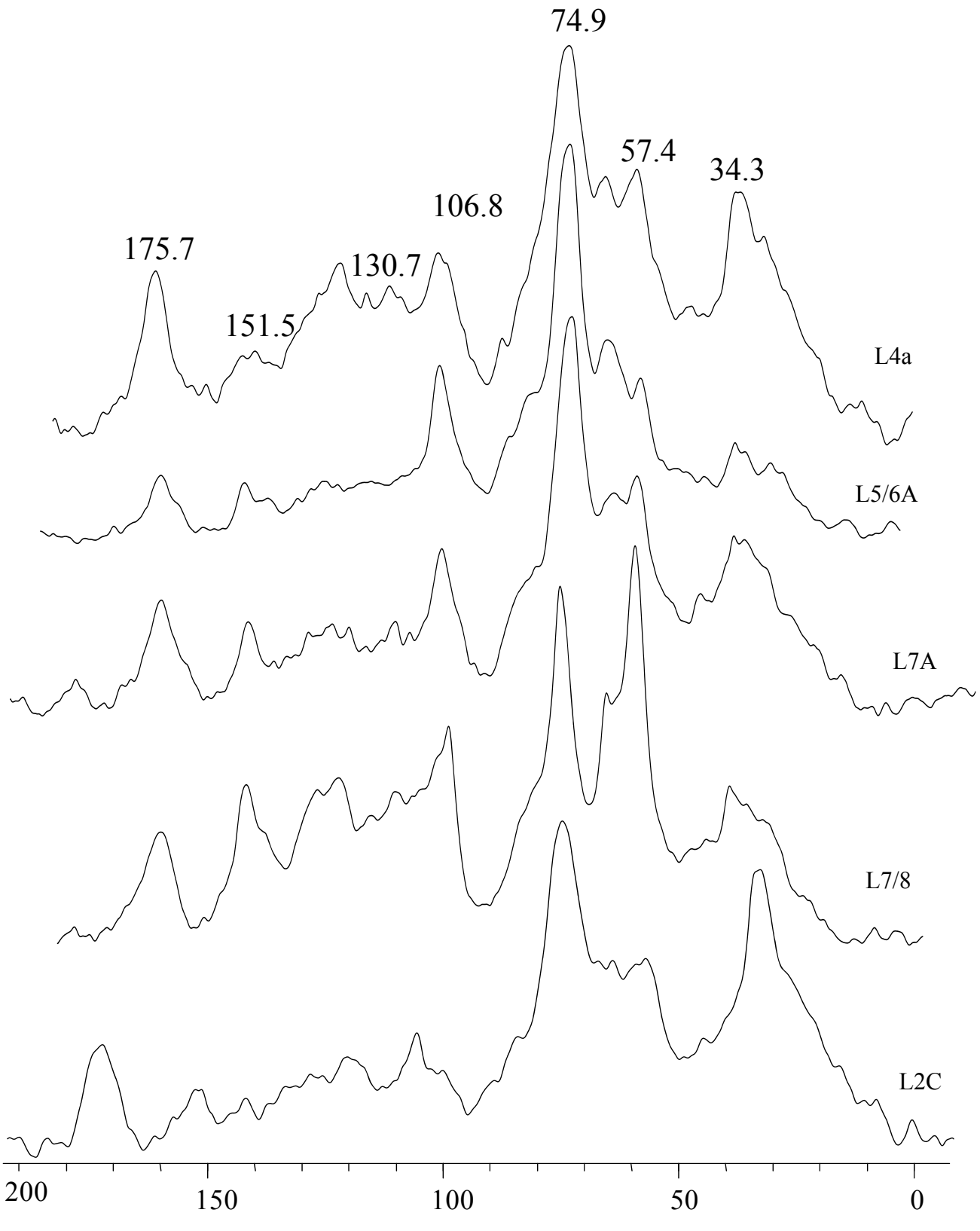

Figure 5c 13C CPMAS spectra of mature compost

3.3.2 off-line TAHM-GC-MS

The list in Table 7 show the representative monomers release by thermochemolysis analyses, while the data in Tables 8 show the yield of main molecular components found in organic materials.

The thermochemolysis applied to bulk compost samples, released more than hundred recognizable different molecules, which were identified as methyl ethers and esters of natural compounds (Table 7), mainly represented by lignin derivatives, fatty acids, aliphatic biopolymers, hydrocarbons and alcohols. Amount and distribution of the most representative monomers were comparable with previous results obtained from the thermochemosys of different organic biomasses. In respect to NMR data, a significant lower yield of carbohydrates was found among the pyrolysis products of compost samples. This finding has been related to the lower efficiency of pyrolysis techniques to detect carbohydrate units of polysaccharides in complex matrices. The thermal behavior and pyrolitic rearrangement of poly-hydroxy components, combined with the alkaline reaction condition of TMAH reagent solution, are believed to negatively interfere in the release and subsequent chromatographic detection of carbohydrates and polysaccharides.

The identified lignin constituents (Table 7) are associated with current symbolism applied in thermochemolysis analysis to identify lignin basic structures: P, p-hydroxyphenyl; G, guaiacyl (3-methoxy, 4-hydroxyphenyl); and S, syringyl (3,5-dimethoxy, 4-hydroxyphenyl). As expected from the initial composition of starting biomasses, the even contribution of the three different forms of lignin components to pyrolitic products indicated both herbaceous and woody tissues of angiosperm species as main sources of organic lignin materials (Table 7). This finding was confirmed by the prevalence, as most representative monomer, of the propenoic acid derivative [2-propenoic acid, 3-(4-methoxyphenyl)-methyl ester] (P18), which is a basic component of lignified tissues of annual crops and grasses.

An increase was found, in each mature compost samples, for the global yield of lignin compounds, with respect to initial biomasses (Table 8), thereby confirming the occurrence of selective preservation of aromatic and phenolic components in the OM stabilization process highlighted by NMR analyses. The extent of lignin preservation or decomposition may be estimated by structural indexes that are based on the relative amount of specific thermochemolysis products associated with the presence of, either, microbially processed organic materials or to undecomposed plant debris. In particular, the aldehydic (G4 and S4) and acidic (G6 and S6) forms of guaiacyl and siryngyl components derive from the progressive degradation of lignin polymer, involving the ongoing oxidation of propyl chain. Conversely the corresponding homologues with integral hydroxylated side chains (G14/15, S14/15) are indicative of unaltered lignin components, which retain the typical β-O-4 ether intermolecular linkages (Table 7). Therefore the indexes obtained (Table 4) by dividing the amount found for the acidic structures over that of, respectively, G4 and

S4 aldehydes (Ad/AlG = G6/G4, Ad/AlS = S6/S4) and for the global yield of threo/erythro isomers (ΓG = G6/[G14 + G15]; ΓS = S6/[S14 + S15]) are regarded as suitable indicators of the bio-oxidative transformation of lignin polymers. The larger the values of dimensionless indexes, the wider the decomposition process of lignin substrates. The lower intensity and the substantial evenness shown by the decomposing indexes, determined at initial and final composting time (Table 8), further indicated an overall maintenance and preservation of hydrophobic aromatic and phenolic constituents.

Aliphatic and alicyclic lipid compounds were the principal alkyl components found in the pyrograms of compost samples (Table 7). The most abundant products were the methyl ester of linear fatty acids, dominated by the hexadecanoic and octadecanoic saturated and unsaturated homologues. These compounds may derive from the breakdown of long chain ester as well as from the terminal oxidation of linear hydrocarbons and aliphatic alcohols. Notwithstanding the multiple possible origins of the C16 and C18 acids, the amount of unsaturated monomers suggested the plant lipids as prevalent source of the straight chain aliphatic acids. The offline pyrolysis of initial biomass, produced also a notable yield of the methylated form of ω–hydroxy alkanoic acids and alkan-dioic acids (Tables 7 and 8). These molecules are the main building blocks of the external hydrophobic protective barriers of fresh and lignified plant tissues, namely cutin and suberin. No clear predominance of particular monomer was revealed by both of these compound classes, which instead showed an almost uniform distribution of even carbon-numbered long chain components (Table 7). Conversely, the di- and tri-hydroxy substituent of the C16 and C18 homologues were the unique representatives of mid-chain-hydroxy alkanoic acids (Tables 7 and 8). The 9,16-/10,16-dihydroxyhexadecanoic isomers, and the 9,10 epoxide 18hydroxy-octadecanoic acid were the most abundant released monomers of these important structural units of plant cuticles, frequently used also as plant biomarkers. The bio-polyesters may also contribute to the large content of the substituted aromatic acids (P18 and G18) found in initial and final compost samples.

The relatively least abundant lipid compounds were the high molecular weight tetra- and pentacyclic triterpenes (Tables 7 and 8), that have been tentatively identified as methyl ethers and esters of both methyl/ethyl cholest(di)en-3-ol structures, and of ursane, lupeane and oleanane derivatives.

The contribution of microbial input was shown by the pyrolytic release of phospho-lipid fatty acids (PLFA) and 2-hydroxy aliphatic acids, which are basic structural components of microbial cells (Table 3). The most representative PLFA monomers were, in order of elution, the 12- and 13-methyl tetradecanoic (iso/anteiso pentadecanoic), the 14- and 15-methyl hexadecanoic (iso/anteiso heptadecanoic) acids and the cyclopropane-(2-hexyl)-octanoic acid (C17 cy FAME), commonly found as characteristic microbial markers of natural organic matter.

As noted for the aromatic derivatives also the relative amount of lipid alkyl molecules of final compost sample, showed a relative increase of about the 50% on total dry weight basis, revealing a differential behaviour for different compound classes (Table 8). The decrease found for linear fatty acids may be attributed to the decomposition of bio-available free components, which undergo to a most favourable decomposition during the active phase of composting processes. Conversely a large preservation was found for the hydrophobic and structural recalcitrant biopolyester constituents, made up by hydroxyl and alkyl dioic acids (Table 8), which form the stable alkyl fraction of the inert SOM pools and may play an important role in determine the bioactivity of compost materials.

Table 7. Main hermochemolysis products released by bulk composts

R.t.[a]	Assignment[b]		R.t.	Assignment	
6.8	2-CH_3O phenol	Carb.	19.9	Benzaldehyde, 3,4,5-triCH_3O	Lig S4
7.5	CH_3O benzene	Lg P1	20.6	*cis*-2-(3,4-DiCH_3Ophenyl)-1-CH_3O ethylene	Lg G7
7.8	Benzene, 1,3-diCH_3O	Lg G1	20.9	*trans*-2-(3,4-DiCH_3Ophenyl)-1-CH_3O ethylene	Lg G8
8.0	Benzene, 1-Ethenyl-4- CH_3O	Lg P3	22.1	*trans* 2-Propenoic acid, 3-(4-CH_3O Phenyl) M.e.	LgP18
9.9	3,4-diCH_3O Toluene	Lg G2	23.1	Benzoic acid, 3,4,5-triCH_3O M.e.	Lg S6
10.1	Phenol, 3,5-diCH_3O	Carb	23.6	*trans*-1-(3,4-DiCH_3O phenyl)-3-CH_3O-1-propene	LgG13
10.8	1H-Indole, 1-Methyl-	N der	24.5	cis-1-(3,4,5-triCH_3O phenyl)-2-CH_3O ethylene	Lg S7
11.8	1,3,5-triCH_3O Benzene	Carb	24.8	C15 *iso* FAME	Mic.
12.1	2-CH_3O-4-Vinylphenol	Lg G3	24.9	threo/erythro-1-(3,4-diCH_3O phenyl) -1,2,3-triCH_3O propane	LgG14
12.5	Carbohydrates derivative	Carb.	24.9	C15 *anteiso* FAME	mic
13.2	Carb.	Carb	25.0	cis-1-(3,4,5-Tri CH_3O phenyl)-2- CH_3O ethylene	Lig S8
13.4	Benzene, 4-Ethenyl-1,2-diCH_3O	Lg G3			
13.5	1,2,3- CH_3O Benzene	Lg S1	25.2	threo/erythro-1-(3,4-Di CH3O phenyl) -1,2,3-tri CH3O propane	LgG15
13.7	Benzoic acid, 4-CH_3O M.e.	Lg P6	25.5	cis-1-(3,4,5-tri CH_3O phenyl)-1- CH_3O -1-propene	LgS11
13.9	2-Propenoic acid, 3-Phenyl M.e.	Biop.	25.7	C15 *n*-FAME	lip
14.2	Benzene, 1,2,3-triCH_3O-5-Methyl	Lg S2	26.1	isomer of G14	Lg G
15.5	4-CH_3O-1-Methylindole	N der.	27.4	2-Propenoic acid, 3-(3,4-diCH_3O Phenyl) M.e.	LgG18
15.7	*trans* Phenol, 2-CH_3O-4-(1-Propenyl)	Lg G	27.5	trans-1-(3,4,5-tri CH_3O phenyl)-3- CH_3O -1-propene	LgS13
16.7	Benzaldheyde 3, 4 diCH_3O	Lg G4	27.6	threo/eryth-1-(3,4,5-triCH_3O phenyl) -1,2,3-triCH_3O propane	LgS14

16.9	Benzene, 1,2-diCH_3O-4-(1-Propenyl)	Lg G21	27.9	threo/erythro-1-(3,4,5-triCH_3O phenyl) -1,2,3-triCH_3O propane	LgS15
17.4	3,4,5-triCH_3O Styrene	Lg S3	28.3	C16 FAME	Lip
17.6	C12 FAME		29.8	C17 iso FAME	Mic.
17.8	Benzenepropanoic acid, 4-CH_3O M.e.	LgP12	30.0	C17 anteiso FAME	Mic
19.0	Ethanone, 1-(3,4-diCH_3O Phenyl)	Lg G5	30.5	cis-1-(3,4,5- triCH_3O phenyl) -1,3-diCH_3O prop-1-ene	LgS16
19.5	*cis* 2-Propenoic acid, 3-(4-CH_3O phenyl)-, M.e.	LgP18	30.6	C17 n FAME	Lip.
			31.4	Carbohydrates derivative	Carb.
19.7	Benzoic acid, 3,4-diCH_3O M.e.	Lg G6	32.3	C18:1 FAME	Lip.

Table 3. Continue

R.t.[a]	Assignment[b]		R.t.	Assignment	
32.4	C18:1 FAME	Lip	44.4	C27 alkane	Lip.
33.0	C18 FAME	Lip.	45.0	C24 FAME	Lip.
33.5	C16 □CH3O FAME	Biop	45.5	C22 ωCH3O FAME	Biop
33.8	C19 br. FAME	Mic.	46.2	C28 alkane	Lip.
34.5	C22 alkane	Lip.	46.3	squalene	Lip.
34.8	C19 cyclopropane FAME	Mic.	46.7	C26 alcohol	Lip.
35.7	C16 dioc acid DIME	Biop	47.0	C24 2 CH_3O FAME	Mic
36.1	Labd-7-en-15-oic acid, 6-oxo-, M.e.	Lip	47.2	C 22 dioic acid DIME	Biop
			47.3	sterol	Lip.
36.4	C16 (9)10-16 diCH_3O FAME	Biop.	47.9	C29 alkane	Lip.
36.7	C23 alkane	Lip.	48.4	C26 FAME	Lip.
36.8	Carbohydrates derivative	Carb	48.9	C24 ωCH3O FAME	Biop
37.2	C18:1 ωCH3O Fame	Biop.	49.0	sterol	Lip.
37.2	C20 FAME	Lip.	49.4	sterol	Lip.
37.8	C16 diCH3O FAME	Biop.	49.6	C30 alkane	Lip.
38.7	C24 alkane	lip	49.8	sterol	Lip.
39.1	Carbohydrates derivative	Carb.	50.1	C28 alcohol	Lip.
39.2	C18:1 dioic acid DIME	Biop	50.6	sterol	Lip.
39.4	C18 12,13-Epoxy-18-CH_3O, FAME	Biop	51.1	C24 dioic acid DIME	Biop
40.7	C25 alkane	Lip.	51.7	C28 FAME	Lip.
41.2	C22 FAME	Lip.	52.0	sterol	Lip.
41.8	C20 ωCH_3O FAME	Biop	52.2	C26 ωCH3O FAME	Biop.
42.1	C18 diCH_3O FAME	Biop	52.7	sterol	Lip.
42.6	C26 alkane	Lip.	53.1	sterol	Lip.
43.1	C23 FAME	Lip.	53.4	sterol	Lip.
43.3	C18 tri CH_3O FAME	Biop			
44.4	C27 alkane	Lip.			

a Rt Retention time (min)

b Biop.= biopolymers; Carb. = Carbohydrates; CH_3O = methoxy; DIME= dimethyl ester; FAME = fatty acid methyl ester; Lg= Lignin; Lip.= lipid; M.e. = methyl ester; Mic. Microbial; N der. = nitrogen compounds;

Table 8. Composition[a] and yields (μg g^{-1}) of TAHM products released from initial biomasses and final composts

Compound	SSMP	CMP	CV t0	CV	L1 t0	L1
Lignin[b]	2190	3470	1710	3230	2123	4946
Ad/Al_G	1.2	0.9	2.4	1.8	2248	4168
Γ_G	1.4	1.5	2.0	1.9	1.2	0.8
Ad/Al_S	2.4	2.7	4.2	3.7	4.5	4.4
Γ_S	1.4	1.3	1.9	1.8	0.9	1.2
Linear FAME C_{12}-C_{30} ($C_{18:1}$)	6820	3740	9575	5740	9540	5420
Microbial FAME C15-C24 (C_{17})	785	889	780	595	1170	895
Hydroxy+ Dioic acids ME C_{16}-C_{26} (C_{16})	1160	3209	2990	3520	2575	4670
Alkanes C_{17}-C_{31}	300	418	252	350	570	995
Alcohols C_{22}-C_{26}	135	92	757	420	1950	900
Sterols	100	195	440	360	230	470

a Total range varying from Ci to Cj; compounds in parentheses are the most dominant homologues; numbers after colon refer to double bond.

b Structural indices: Ad/Al = G6/G4, S6/S4; ΓG = G6/(G14 + G15); ΓS = S6/(S14 + S15).

Table 8. Composition[a] and yields (μg g^{-1}) of TAHM products released from initial biomasses and final composts

Compound	L2 t0	L2	L3 t0	L3	L4 t0	L4
Lignin[b]	2248	4168	1912	4157	2123	4946
Ad/Al_G	1.2	0.8	1.9	2.0	1.0	0.9
Γ_G	4.5	4.6	2.6	3.6	2.7	3.1
Ad/Al_S	3.8	2.8	2.1	2.2	3.0	2.5
Γ_S	0.5	0.3	1.2	1.4	1.1	0.9
Linear FAME C_{12}-C_{30} ($C_{18:1}$)	9575	4820	10672	7820	8540	4210
Microbial FAME C15-C24 (C_{17})	995	573	875	780	960	540
Hydroxy+ Dioic acids ME C_{16}-C_{26} (C_{16})	1949	4909	2309	4715	2520	3510
Alkanes C_{17}-C_{31}	975	850	450	395	740	580
Alcohols C_{22}-C_{26}	1120	850	950	640	1620	960
Sterols	210	145	250	185	220	150

a Total range varying from Ci to Cj; compounds in parentheses are the most dominant homologues; numbers after colon refer to double bond.

b Structural indices: Ad/Al = G6/G4, S6/S4; ΓG = G6/(G14 + G15); ΓS = S6/(S14 + S15).

Table 8. Composition[a] and yields (μg g^{-1}) of TAHM products released from initial biomasses and final composts

Compound	L1A t0	L1A	L2A t0	L2A	L3A t0	L3A
Lignin[b]	3415	4300	1980	2390	2150	3550
Ad/Al_G	2.2	3.0	2.9	2.7	3.2	2.4
Γ_G	4.0	2.8	2.3	1.7	0.8	1.1
Ad/Al_S	2.4	1.4	1.9	2.1	3.2	2.7
Γ_S	1.5	1.5	1.0	1.2	0.7	1.1
Linear FAME C_{12}-C_{30} ($C_{18:1}$)	14751	8535	8690	4560	8750	6220
Microbial FAME C15-C24 (C_{17})	436	399	985	680	1120	915
Hydroxy+ Dioic acids ME C_{16}-C_{26} (C_{16})	2470	5800	1620	4110	2115	3980
Alkanes C_{17}-C_{31}	540	255	250	280	360	295
Alcohols C_{22}-C_{26}	1120	980	1475	1040	1212	850
Sterols	250	185	420	90	550	350

a Total range varying from Ci to Cj; compounds in parentheses are the most dominant homologues; numbers after colon refer to double bond.

b Structural indices: Ad/Al = G6/G4, S6/S4; ΓG = G6/(G14 + G15); ΓS = S6/(S14 + S15).

Table 8. Composition[a] and yields (μg g^{-1}) of TAHM products released from initial biomasses and final composts

Compound	L4A t0	L4A	L5/6 t0	L5/6	L7/A t0	L7A
Lignin[b]	1960	3473	2670	3620	2980	4270
Ad/Al_G	2.6	2.1	4.2	3.7	2.8	1.9
Γ_G	1.6	1.9	0.7	1.1	2.1	1.6
Ad/Al_S	2.9	2.3	3.5	2.6	2.7	2.2
Γ_S	0.7	0.8	1.2	1.4	0.9	0.7
Linear FAME C_{12}-C_{30} ($C_{18:1}$)	8540	5420	6540	4850	11085	8750
Microbial FAME C15-C24 (C_{17})	650	480	865	540	470	465
Hydroxy+ Dioic acids ME C_{16}-C_{26} (C_{16})	3620	8200	2985	4500	2750	5345
Alkanes C_{17}-C_{31}	890	1100	850	645	650	250
Alcohols C_{22}-C_{26}	2200	1850	685	780	755	590
Sterols	230	195	125	190	360	285

a Total range varying from Ci to Cj; compounds in parentheses are the most dominant homologues; numbers after colon refer to double bond.
b Structural indices: Ad/Al = G6/G4, S6/S4; ΓG = G6/(G14 + G15); ΓS = S6/(S14 + S15).

Table 8. Composition[a] and yields (μg g^{-1}) of TAHM products released from initial biomasses and final composts

Compound	L7/8 t0	L7/8	L2C t0	L2C
Lignin[b]	2190	4470	1980	3390
Ad/Al_G	1.2	0.9	1.4	1.2
Γ_G	4.0	2.8	2.3	1.7
Ad/Al_S	2.4	2.7	2.9	2.5
Γ_S	1.3	1.3	0.8	1.1
Linear FAME C_{12}-C_{30} ($C_{18:1}$)	4760	3820	6590	4870
Microbial FAME C15-C24 (C_{17})	960	790	690	480
Hydroxy+ Dioic acids ME C_{16}-C_{26} (C_{16})	2150	3290	1680	4110
Alkanes C_{17}-C_{31}	540	255	250	280
Alcohols C_{22}-C_{26}	530	270	675	440
Sterols	210	115	195	220

a Total range varying from Ci to Cj; compounds in parentheses are the most dominant homologues; numbers after colon refer to double bond.
b Structural indices: Ad/Al = G6/G4, S6/S4; ΓG = G6/(G14 + G15); ΓS = S6/(S14 + S15).